INTERNATIONAL JOURNAL OF AUTOMOTIVE AND MECHANICAL ENGINEERING (IJAME)
ISSN: 2229-8649 e-ISSN: 2180-1606
VOL. 18, ISSUE 2, 8658 – 8667
DOI: https://doi.org/10.15282/ijame.18.2.2021.03.0659

ORIGINAL ARTICLE

Effect of Increasing Spindle Speed at a Constant Chip Load on Cutting Force Behaviour of Hastelloy X

N.A. Mohd Nor[1*], B.T.H.T. Baharudin[1], J.A. Ghani[2], M.K.A. Mohd Ariffin[1], Z. Leman[1], N. Ismail[1] and A. Ginting[3]

[1]Department of Mechanical and Manufacturing Engineering, Faculty of Engineering, Universiti Putra Malaysia, 43400 Serdang, Malaysia
[2]Department of Mechanical and Materials Engineering, Faculty of Engineering and Built Environment, Universiti Kebangsaan Malaysia, 43600 Bangi, Malaysia
[3]Department of Mechanical Engineering, Faculty of Engineering, Universitas Sumatera Utara, 20222 Sumatera Utara, Indonesia

ABSTRACT – Cutting force is vital in machining nickel-based superalloys due to their excellent mechanical properties, thus creating difficulty in cutting. In the current scenario of metal machining, milling processes require high spindle speed and low chip load, which result in a low cutting force. However, low chip load not only result in low cutting force but also result in a low material removal rate (MRR). It is contrary to the ultimate high-speed machining (HSM) goal, which is to improve productivity and cost-effectiveness. Therefore, the emergence of an approach for achieving simultaneous low cutting force and high MRR is crucial. This paper presents the effect of increasing spindle speed at a constant chip load on the cutting force of Hastelloy X during half-immersion up-milling and half-immersion down-milling. In both half-immersions, the simulation results and experimental results are in good agreement. The percentage contribution of feed force, normal force and axial force to the resultant force can be arranged descendingly from high to low as axial force > normal force > axial force. Moreover, feed force, normal force, axial force and resultant force have a U-shaped behaviour. The spindle speed of 24,100 rpm and a chip load of 0.019 mm/tooth were found to achieve both low cutting force and high MRR.

ARTICLE HISTORY
Received: 4th Dec 2020
Revised: 22nd Feb 2021
Accepted: 4th May 2021

KEYWORDS
Spindle speed;
Chip load;
Cutting force;
Hastelloy X;
Half-immersion

INTRODUCTION

Cutting force issues are frequently encountered in the aerospace manufacturing industry due to nickel-based superalloys that tend to be more difficult to machine compared to other traditional materials. Hastelloy X or Inconel HX is one of the most widely used nickel-based superalloys for aerospace components, such as structure [1] and gas turbine engines for the combustion zone components [2-5]. Taking into consideration that aerospace components have to accomplish certain temperature and oxidation resistance [1-5], it has helped to drive demand for this superalloy. Moreover, eliminating the excessive cutting force during Hastelloy X machining has become a constant pressure on aerospace manufacturers. The ability to eliminate excessive cutting force can contribute not only to the quality of machined materials [6-10] and extend the cutting tool life [6, 7], but also can minimise the rate of production cost [8] and maximise productivity [9, 10]. Cutting force is commonly divided into three components, which are feed force, normal force and axial force [8]. These cutting force components can be accurately measured by strain gauge sensors [8] or piezoelectric sensors [8, 10] embedded in the dynamometer. On the other hand, the cutting force can also be predicted via Finite Element Method (FEM) techniques by analysing chip formation in metal machining [11].

Meanwhile, research on cutting force stated that a decrease in cutting force coincides with an increase in cutting speed [11-15]. This is attributed to the generation of higher cutting temperature in the shear zone, which soften the machined material owing to a drop in its mechanical properties [13, 14]. Spindle speed is correlated to cutting speed. Thus, the increase in spindle speed during metal machining will not only increase cutting speed but also increases MRR. On the other side, an incremental decrease in feed rate leads to a gradual decrease in cutting force [6, 16, 17]. In the feed rate perspective, as chip load decreases, the cutting force also decreases due to cutting tool contact with the machined material and unwanted machined material that require removal decrease [6]. In fact, the MRR is tied to the feed rate. Therefore, decreasing the chip load not only decrease the feed rate but can also decrease the cutting force, which can indirectly reduce the MRR as well. It can be summarised that the variation of spindle speed value and chip load value during metal machining has a different effect on cutting force behaviour but has the same effect on MRR behaviour.

As a current practice in the aerospace manufacturing industry, the end-milling process requires high spindle speed and low chip load, which result in low cutting force. Apart from this, it contradicts the HSM goal, in which an increase in cutting speed and feed rate is the primary method used to increase MRR, with the purpose of improving productivity and cost-effectiveness [12]. Since MRR is directly proportional to both spindle speed and chip load while cutting force has different kinds of proportionality to both cutting parameters; thus a new approach not only guaranteeing low cutting force but must also exist in high MRR. Apart from this, a precise understanding of the influence of an increase in spindle

*CORRESPONDING AUTHOR | N. A. Mohd Nor | ✉ noraznan.namn@gmail.com

speed value at different constant chip load values on the cutting force is vital. This paper elucidates an effect of the increase in spindle speed at a constant chip load on the cutting force of ASME SB435 Hastelloy X plate during half-immersion up-milling and half-immersion down-milling by simulation test. This nickel-based superalloy is used extensively as a material for the combustion chamber in a gas turbine engine [4]. Further, the percentage contribution of each cutting force component to resultant force and the behaviour of cutting force components and the resultant force was analysed systematically. Moreover, the optimal cutting condition for achieving low cutting force and high MRR is simultaneously proposed. Finally, simulation results were validated by experimental results.

PROCEDURE

A simulation test of increasing the spindle speed at a constant chip load on Hastelloy X cutting force was done using the Third Wave Systems Advant Edge software. The three dimensional (3D) cutting systems were simulated in a dry condition using a constant depth of cuts, while the values of spindle speed and chip load varied, as shown in Table 1. The increment of spindle speed was 2700 rpm. Additionally, the variable cutting parameters were selected by taking into consideration ISO 3002/4 standard as proposed by Kennametal.

Table 1. Variable cutting parameters used in the simulation test

Cutting parameter	Value
Spindle speed (rpm)	13,300 to 37,600
Chip load (mm/tooth)	0.013, 0.016, and 0.019
Depth of cut (mm)	0.2

The STL file of KYS40 solid ceramic end-mill cutter diameter of 6 mm with 4 flutes was provided by the Kennametal. It was imported into the software to perform the Hastelloy X half-immersion up-milling and half-immersion down-milling. The hardness of Hastelloy X was 92 HR_B with a length of 90 mm, width of 6 mm and thickness of 2 mm. The mechanical properties of Hastelloy X and the meshing parameters used in the simulation tests are presented in Table 2 and Table 3. In addition, the selected value of meshing parameters was based on the cutting force results obtained from the preliminary simulation test, which is similar to the initial experimental test.

Table 2. Mechanical properties of Hastelloy X used in the simulation test.

Mechanical property	Value
Tensile strength (MPa)	792.9
Yield strength (MPa)	344.7
Elongation (%)	45.5

Table 3. Meshing parameters used in the simulation test.

Meshing parameter	Value
Maximum element size (mm)	1
Minimum element size (mm)	0.15
Mesh grading	0.5
Curvature safety	2.5
Segmented per edge	2
Minimum edge length (mm)	0

Cutting force components consist of feed force, normal force, and axial force – all of which were recorded during increasing spindle speed at a chip load of 0.013 mm/tooth and depth of cut of 0.2 mm. The method was repeated by changing a chip load of 0.013 mm/tooth to 0.016 mm/tooth, followed by a chip load of 0.016 mm/tooth to 0.019 mm/tooth. From the recorded cutting force components, the resultant force was computed using Eq. (1) below.

$$Fr = \sqrt{Fx^2 + Fy^2 + Fz^2} \tag{1}$$

Afterwards, the cutting force components and resultant force were analysed in terms of the percentage contribution of each cutting force component to the resultant force, as well as the behaviour of cutting force components and resultant force from the obtained trend-line by using an X-Y plot in Microsoft Excel. Furthermore, the desirability function analysis (DFA) was adopted in Minitab software for the purpose of proposing the optimal cutting condition for achieving low cutting force and high MRR simultaneously, during half-immersion up-milling and half-immersion down-milling of Hastelloy X.

The proposed optimal cutting condition was also validated by comparing the value of cutting force components and resultant force obtained from the simulation test with the value of cutting force components and resultant force obtained from the experimental test. Table 4 shows the variable cutting parameters used in the experimental test. The total run was set at six runs for both half-immersions. The chip load was set to vary at 0.013 mm/tooth, 0.016 mm/tooth and 0.019

mm/tooth, while the spindle speed and depth of cut were held constant at 24,100 rpm and 0.2 mm respectively. The variable cutting parameters were selected based on DFA results with high D values.

Table 4. Variable cutting parameters used in the experimental test

Cutting parameter	Value
Spindle speed (rpm)	24100
Chip load (mm/tooth)	0.013, 0.016, and 0.019
Depth of cut (mm)	0.2

Half-immersion up-milling and half-immersion down-milling of Hastelloy X were conducted on a Mori Seiki NV4000 DCG machining centre which has a maximum spindle speed of 30000 rpm. The same machined material and end-mill cutter of simulation test were used in the experimental test. In addition, a new end-mill cutter was used at each run so that tool wear could be neglected. Cutting force components were recorded using Dynamometer Type 9129AA from Kistler and was repeated three times to find the average. The recorded cutting force components at each run were inserted into Eq. (1) to obtain the resultant force. Further, cutting force components and resultant force was plotted into clustered column plot in the Microsoft Excel, and then was validated in terms of the percentage contribution of each cutting force component to resultant force and relative error value.

RESULTS AND DISCUSSION

Figure 1 illustrates the sample of simulation result obtained from half-immersion up-milling, where the spindle speed and chip load were set at 13300 rpm and 0.013 mm/tooth. Since all runs in this research only considered the value of cutting force component per flute, thus the values of feed force (red colour), the normal force (green colour) and the axial force (blue colour) in Figure 1 were recorded at a cutting time of 0.00113 s due to the cutting length was set at 0.013 mm. The root mean square (RMS) method was used to obtain the mean value of cutting force components at each run. This is due to the value of feed force, normal and axial force having positive and negative values.

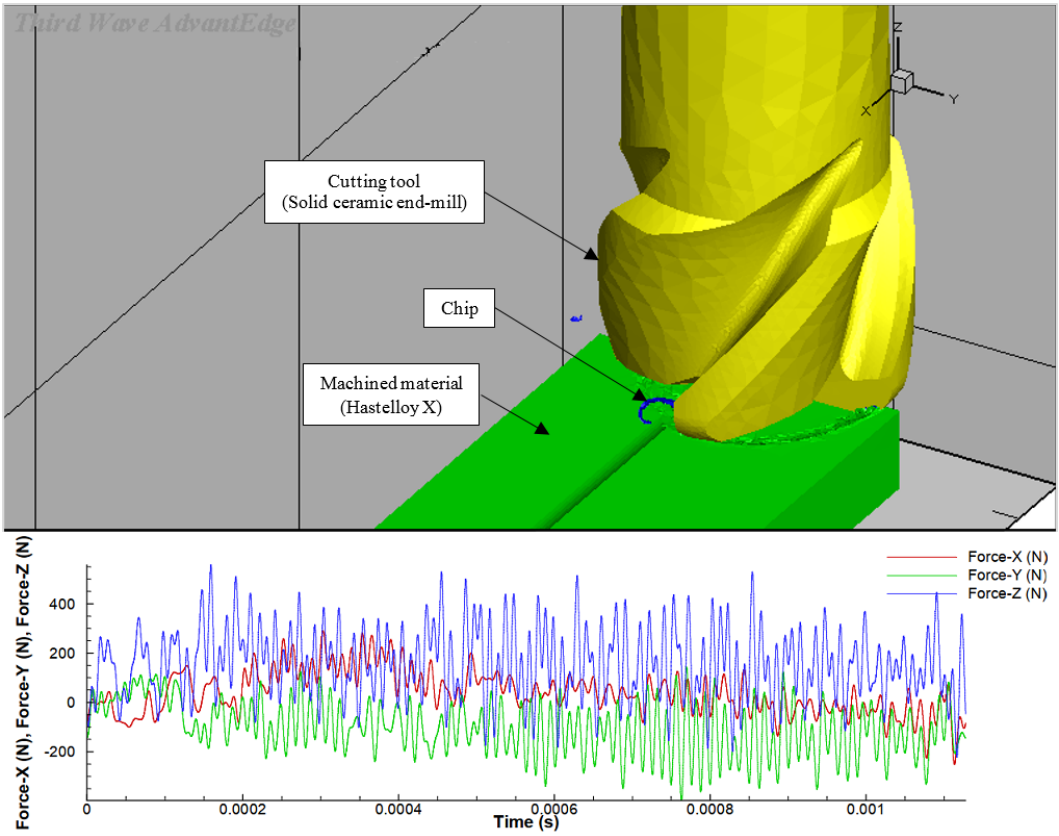

Figure 1. Simulation of half-immersion up-milling.

Afterwards, the mean value of cutting force components for each run was inserted into Eq. (1) to compute the resultant force for each run. The obtained resultant force and the mean value of cutting force components were elucidated via an X-Y plot, as shown in Figure 2 to Figure 5. By observing the results of the cutting force components and resultant force in Figure 2 to Figure 5, the findings indicated that the axial forces dominated a total resultant force with an estimation of 60% during half-immersion up-milling and 51% during half-immersion down-milling. This was significantly higher than the normal force and feed force, which contributed approximately 25% and 15%, respectively, during half-immersion up-

milling, while 33% and 16%, respectively, during half-immersion down-milling. This phenomenon is in line with the findings discovered by Karpuschewski et al. [18] and Mohd Nor et al. [19]. Overall, the axial force appears as the main contributor that influences the resultant force, followed by the normal force and feed force. There are no significant differences between cutting force component values and resultant force values in the half-immersion up-milling compared to the half-immersion down-milling.

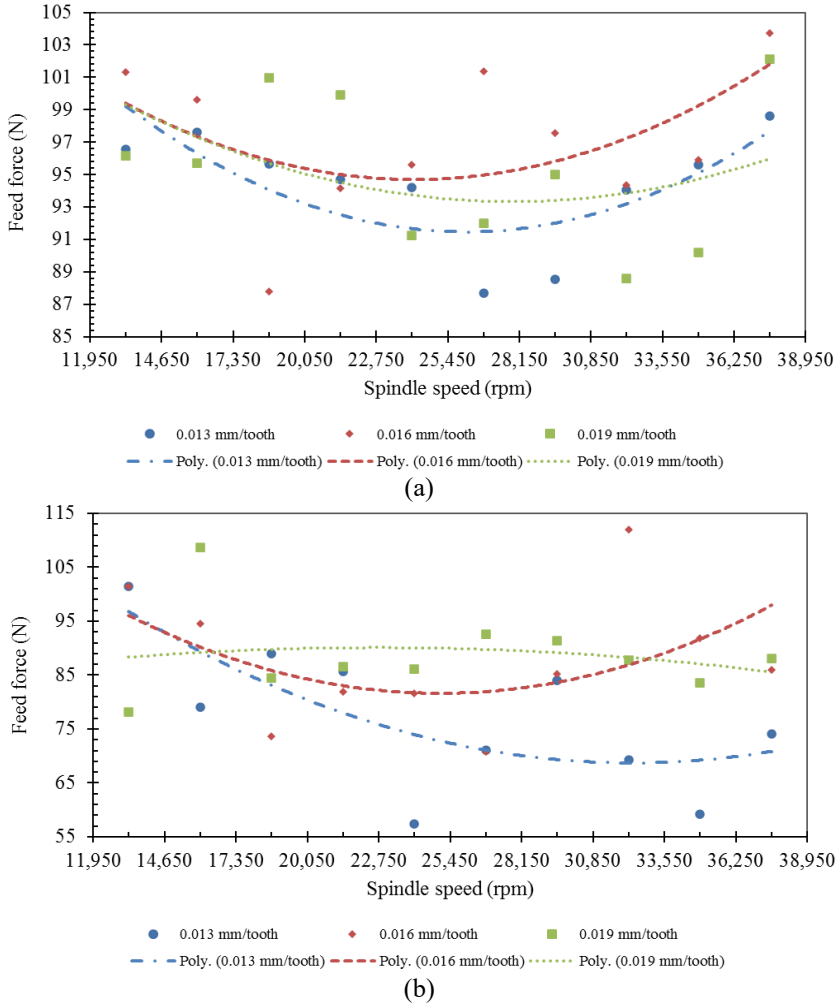

Figure 2. Feed force against spindle speed in (a) half-immersion up-milling and (b) half-immersion down-milling**.**

Needless to say, there are numerous scientific papers that mentioned an incremental increase in spindle speed leads to an incremental reduction in cutting force. However, the X-Y plots in Figure 2 to Figure 5 demonstrated that in both half-immersions, the trend-lines of cutting force components and resultant force had fluctuated as the spindle speed increased from 13300 rpm to 37600 rpm at constant chip loads of 0.013 mm/tooth, 0.016 mm/tooth and 0.019 mm/tooth. Thus it can be claimed that the behaviour of cutting force when the spindle speed increased at the constant chip load is quadratic instead of linear, as previously mentioned in [11-15], where cutting force is defined in a linear relationship with respect to the spindle speed. Besides, the cutting force components and resultant force have quadratic behaviour. Figure 2 to 5 indicate that although the chip load was linearly increased at the constant spindle speed, the behaviour of cutting force components and resultant force fluctuated with an uneven quadratic coefficient. Therefore, it is contrary to the findings indicated by Bolar et al. [6], Tsai et al. [16], and Liu et al. [17], whereby those studies showed that the cutting force decreased as the chip load decreased.

Moreover, it was noticeable that the behaviour of cutting force components and the resultant force initially decreased and subsequently increased after reaching a specific spindle speed. Except for the behaviour of axial force at the chip load of 0.019 mm/tooth during half-immersion up-milling, the feed force behaviour at the chip load of 0.019 mm/tooth, and normal force at chip load of 0.013 mm/tooth during half-immersion down-milling. Therefore, it can be generally stated that cutting force has U-shaped behaviour. Feed force at chip load of 0.013 mm/tooth in half-immersion up-milling and feed force at chip load of 0.016 mm/tooth in both half-immersions (as shown in Figure 2), normal force at chip load of 0.016 mm/tooth and 0.019 mm/tooth in both half-immersions (as depicted in Figure 3), axial force at chip load of 0.013 mm/tooth in both immersions and axial force at chip load of 0.016 mm/tooth in half-immersion up-milling (as presented in Figure 4), and resultant force at chip load of 0.013 mm/tooth and 0.016 mm/tooth in both half-immersions (as illustrated in Figure 5) all had an obvious U-shaped behaviour. Furthermore, the phenomenon in which the cutting force initially decreased and subsequently increased in metal machining might be associated with the ductile-to-brittle transition, which

caused the machined materials to become brittle at a high strain rate or at low temperature due to the material's ability to absorb a specific amount of energy during machining operations [20-23]. In addition, the cutting force for the transition period from the ductile regime to the brittle regime will decrease when the spindle speed is increased. Whereas a cutting force for ductile or brittle regime alone will increase when the spindle speed is increased [20].

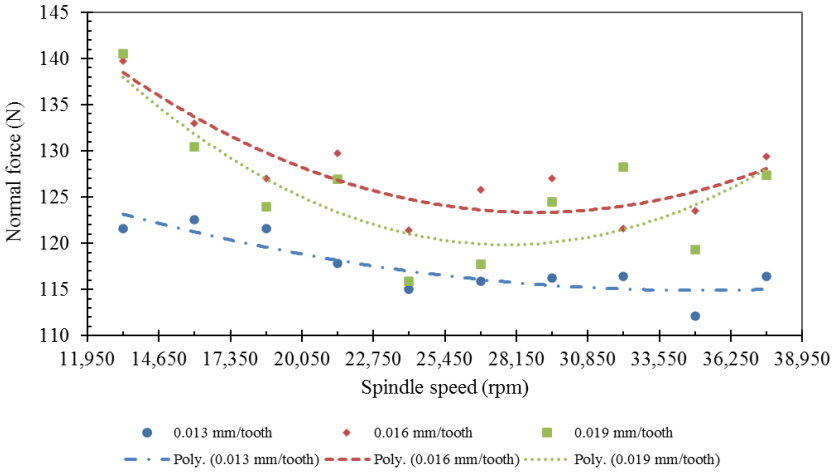

(a)

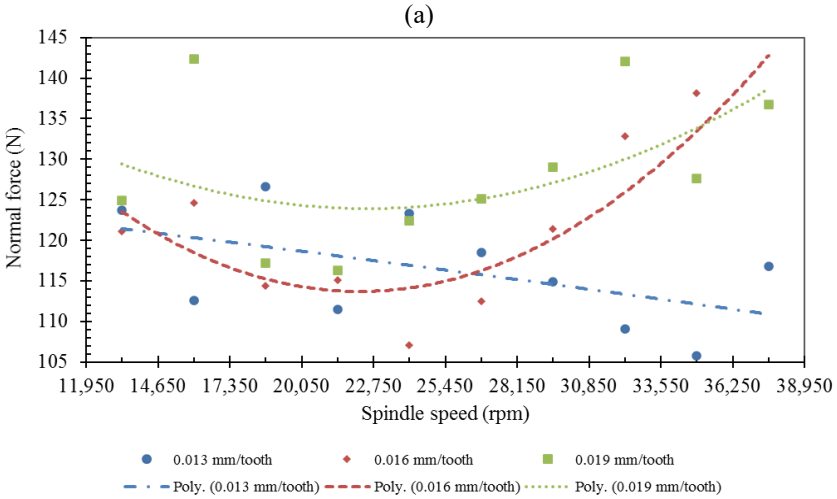

(b)

Figure 3. Normal force against spindle speed in (a) half-immersion up-milling and (b) half-immersion down-milling.

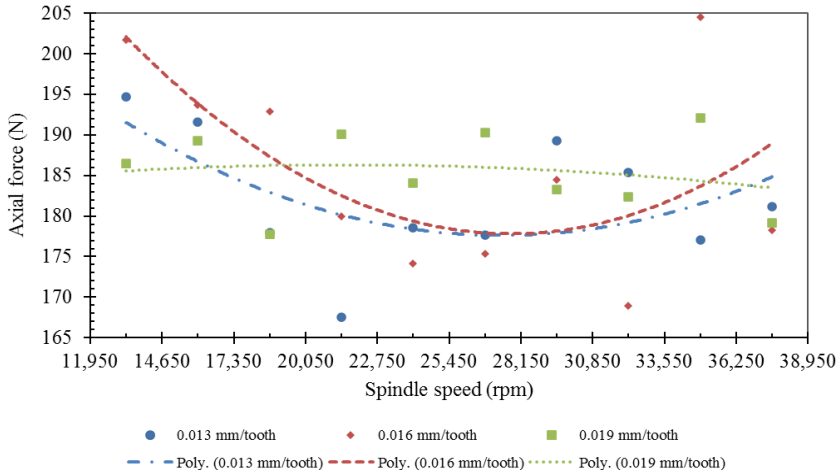

(a)

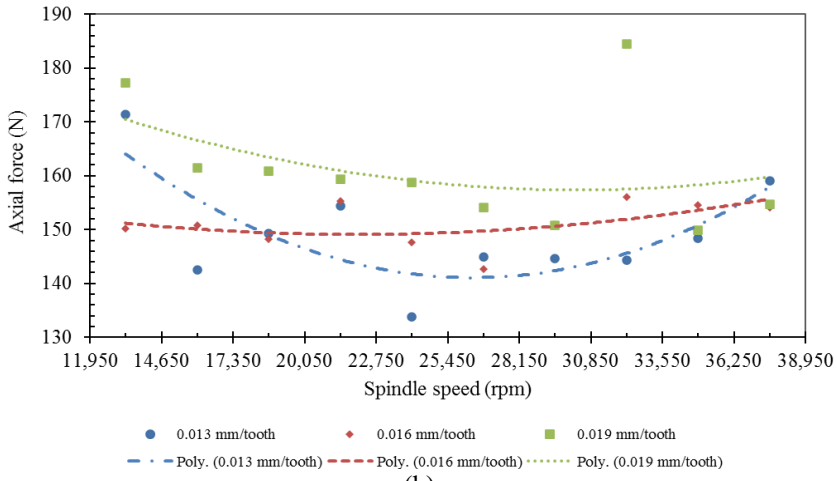

(b)

Figure 4. Axial force against spindle speed in (a) half-immersion up-milling and (b) half-immersion down-milling.

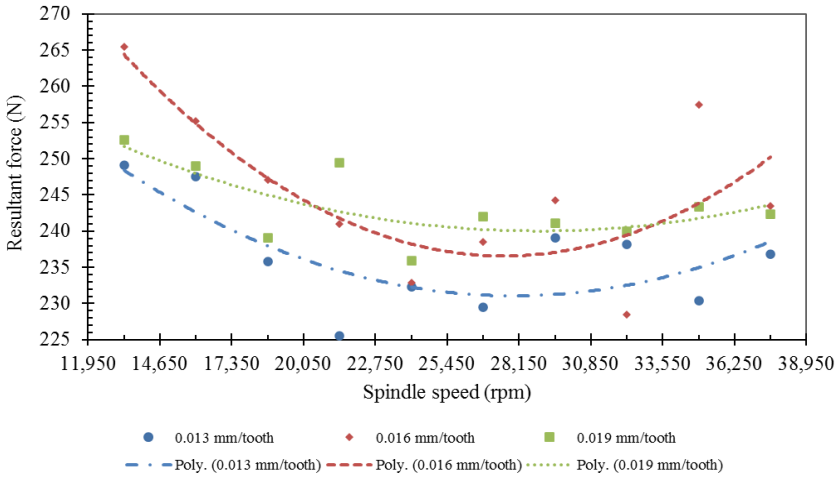

(a)

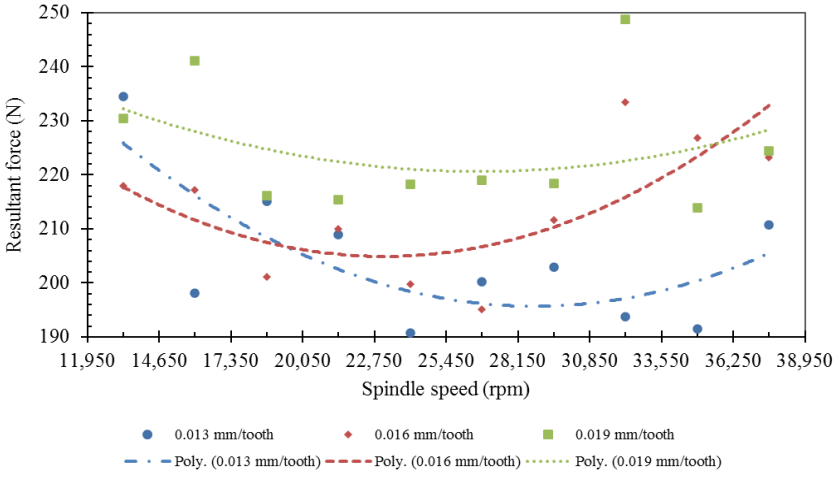

(b)

Figure 5. Resultant force against spindle speed in (a) half-immersion up-milling and (b) half-immersion down-milling.

The optimal cutting condition for achieving low cutting and high MRR can be determined via DFA and subsequently proposed. The optimisation plot in Figure 6 presents the details of DFA results for both half-immersions. This plot determines the influence of each factor (columns) on the responses or composite desirability (rows). The factor consists of spindle speed and chip load, while the response consists of feed force, normal force, axial force and resultant force. In the upper left corner and the top row indicate composite desirability (D) value, while at the left of each response row indicate individual desirability (d) value. The goal is to minimise feed force, normal force, axial force and resultant force in both half-immersions. Additionally, D values that are close to 1.0000 indicate that the combination of spindle speed and chip load achieved favourable results for all responses as a whole.

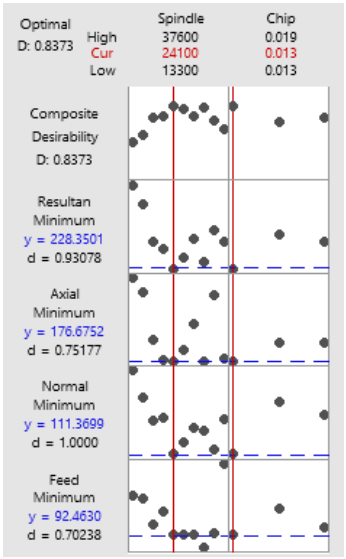

(a) half-immersion up-milling

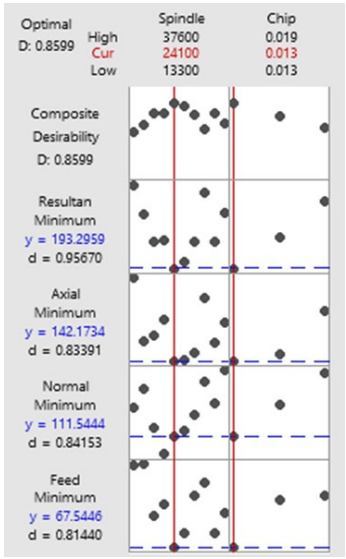

(b) half-immersion down-milling

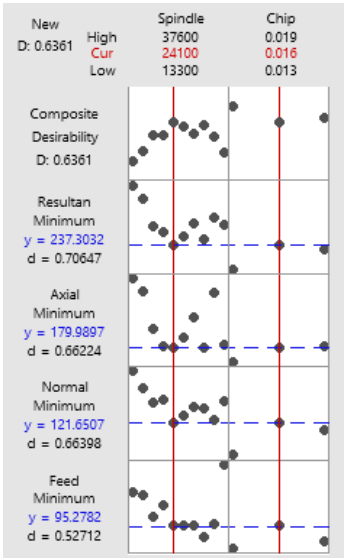

(c) half-immersion up-milling

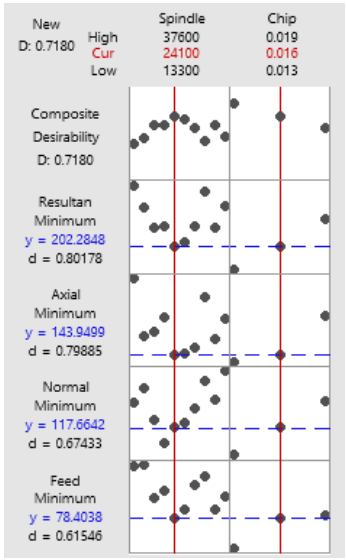

(d) half-immersion down-milling

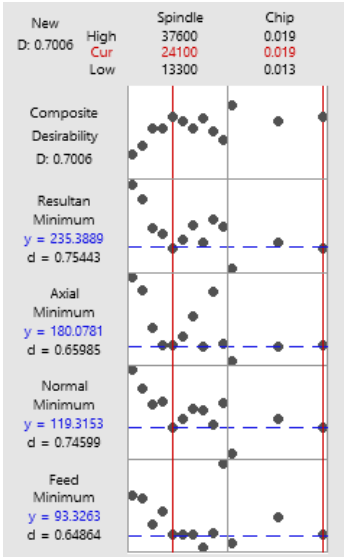

(e) half-immersion up-milling

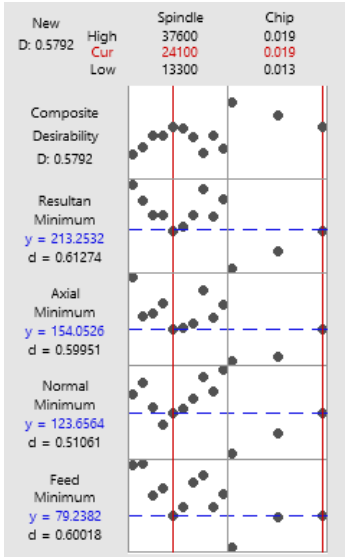

(f) half-immersion down-milling

Figure 6. Optimisation plot at chip load of (a), (b), 0.013 mm/tooth, (c), (d) 0.016 mm/tooth and (e), (f) 0.019 mm/tooth in half-immersion up-milling and down-milling.

From the optimisation plot in Figure 6, DFA results indicated that the spindle speed of 24100 rpm had the highest D value at each level of chip load in both half-immersions. The D values at a spindle speed of 24100 rpm at chip load of 0.013 mm/tooth for half-immersion up-milling and half-immersion down-milling were 0.8373 and 0.8599 respectively, as depicted in Figure 6(a) and 6(b). While at chip load of 0.016 mm/tooth, the D values were 0.6361 and 0.7180 respectively for half-immersion up-milling and half-immersion down-milling, as presented in Figure 6(c) and 6(d). Further, D values of 0.7006 and 0.5792 were obtained for half-immersion up-milling and half-immersion down-milling at chip load of 0.019 mm/tooth as illustrated in Figure 6(e) and 6(f). Since the spindle speed of 24100 rpm has the highest D value at each level of chip load, this indirectly indicates that this spindle speed generates minimum feed force, normal force, axial force and resultant force at a chip load of 0.013 mm/tooth, 0.016 mm/tooth and 0.019 mm/tooth in both half-immersions.

Apart from this, half-immersion up-milling and half-immersion down-milling of Hastelloy X at a spindle speed of 24100 rpm and a chip load of 0.013 mm/tooth could result in the lowest cutting force. Since MRR is proportional to chip load [6], this combination of spindle speed and chip load is suitable for aerospace manufacturers to achieve the lowest cutting force only due to low chip load value. Therefore, for achieving low cutting force and high MRR simultaneously, aerospace manufacturers are proposed to perform half-immersion up-milling and half-immersion down-milling of Hastelloy X at a spindle speed of 24100 rpm and a chip load of 0.019 mm/tooth. This also shows that increasing chip load at a spindle speed of 24100 rpm in both half-immersions can increase MRR while maintaining the cutting force at a relatively low level. In addition, an increase in spindle speed beyond 24100 rpm while decreasing chip load as current practice in metal machining to reduce cutting force becomes an irrelevant approach as the cutting force has U-shaped behaviour.

The cutting force results at a spindle speed of 24100 rpm and accompanied with a chip load of 0.013 mm/tooth, 0.016 mm/tooth and 0.019 mm/tooth in both half-immersions obtained from the simulation test were validated by experimental results. Clustered column plot in Figure 7 illustrates the validation results. The X-axis represents feed force, normal force, axial force and resultant force for simulation test and experimental test, whereas the Y-axis represents cutting force. Furthermore, blue colour, red colour and green colour represent chip load of 0.013 mm/tooth, 0.016 mm/tooth and 0.019 mm/tooth, respectively.

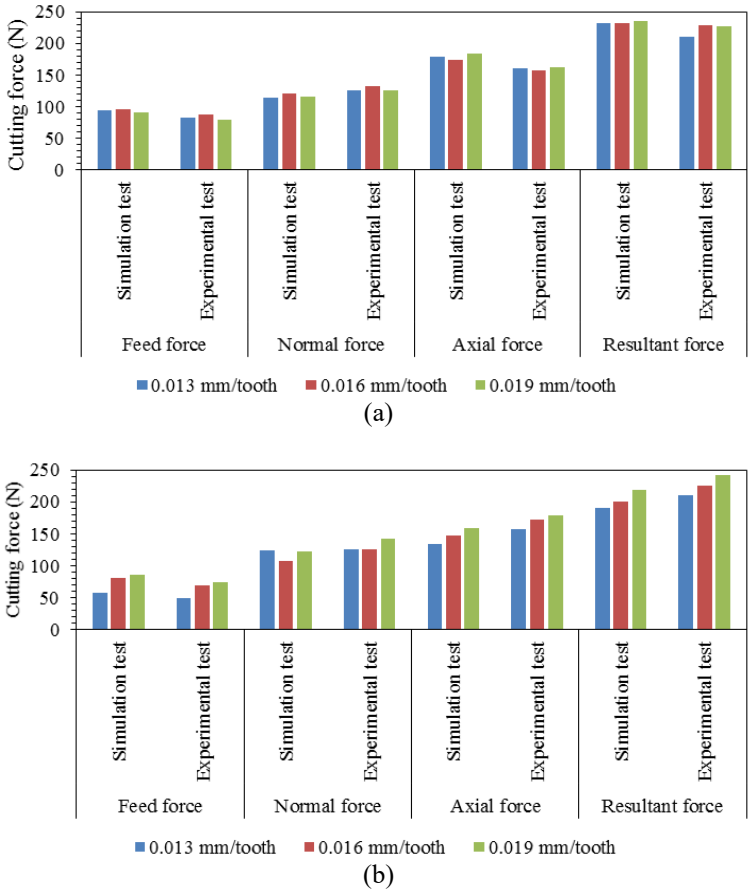

Figure 7. Clustered column plot for (a) half-immersion up-milling and (b) half-immersion down-milling.

From Figure 7, it can be seen that the simulation results in both half-immersions were close to the experimental results in both half-immersions. Experimental results show that axial force dominated a total resultant force, followed by normal force and feed force, thus in line with the simulation results. Furthermore, the relative error of simulation results for both half-immersions was within 15%, indicating that the simulation results and the experimental results were in good agreement [24, 25]. This proves that spindle speed of 24,100 rpm and chip load 0.013 mm/tooth is the optimal cutting

condition for achieving the lowest cutting force in both half-immersions, while spindle speed of 24,100 rpm and a chip load of 0.019 mm/tooth is the optimal cutting condition for achieving low cutting force and high MRR simultaneously in both half-immersions.

CONCLUSION

The effect of increasing spindle speed at a constant chip load on the cutting force of Hastelloy X during half-immersion up-milling and half-immersion down-milling were elucidated. The following conclusions can be drawn from this research:

i. The simulation results agree with experimental results as the relative error is within 15%.
ii. The axial force has a major contribution to the resultant force, followed by normal force and feed force.
iii. The behaviour of feed force, normal force, axial force and resultant force initially decreased and subsequently increased after reaching a specific spindle speed.
iv. The optimal cutting condition for achieving the lowest cutting force can be obtained using a spindle speed of 24100 rpm and a chip load of 0.013 mm/tooth, while the optimal cutting condition for achieving low cutting force and high MRR simultaneously can be obtained using a spindle speed of 24100 rpm and a chip load of 0.019 mm/tooth.
v. Future research should be carried out experimentally to identify the effect on surface integrity based on the proposed optimal cutting condition.

ACKNOWLEDGEMENT

The authors would like to acknowledge the financial support from the Universiti Putra Malaysia under Research Grant no. GP-IPS/2017/9539900. Also, the authors would like to thank Mr Mohd Nor Bin Puteh, Mdm Hatijah Binti Kassim, Mdm Dyg. Siti Quraisyah Bt. Abg. Adenan and Mr Nor Iman Ziqri Bin Nor Aznan for encouragement.

REFERENCES

[1] Chennamsetty ARK, Leblanc J, Abotula S, et al. Dynamic response of Hastelloy® X plates under oblique shocks, Experimental and numerical studies. International Journal of Impact Engineering 2016; 92: 75–88.

[2] Han Q, Gu Y, Soe S, et al. Effect of hot cracking on the mechanical properties of Hastelloy X superalloy fabricated by laser powder bed fusion additive manufacturing. Optics & Laser Technology 2020; 124: 105984.

[3] Wang Han Q, Gu Y, Wang L, et al. Effects of TiC content on microstructure and mechanical properties of nickel-based hastelloy X nanocomposites manufactured by selective laser melting. Materials Science and Engineering 2020; 796: 140008.

[4] Romero-Jabalquinto A, Velasco-Téllez A, Zambrano-Robledo P, Bermúdez-Reyes B. Feasibility of manufacturing combustion chambers for aeronautical use in Mexico. Journal of Applied Research and Technology 2016; 14(3): 167–172.

[5] Oschelski TB, Urasato WT, Amorim HJ, and Souza AJ. Effect of cutting conditions on surface roughness in finish turning Hastelloy® X superalloy. Materials Today: Proceedings 2021; 44: 532-537.

[6] Bolar G, Das A, Joshi SN. Measurement and analysis of cutting force and product surface quality during end-milling of thin-wall components. Measurement 2018; 121: 190–204.

[7] Wei Ma J, Ning Song D, Yuan Jia Z, et al. Tool-path planning with constraint of cutting force fluctuation for curved surface machining. Precision Engineering 2018; 51: 614–624.

[8] Xie Z, Lu Y, Li J. Development and testing of an integrated smart tool holder for four-component cutting force measurement. Mechanical Systems and Signal Processing 2017; 93: 225–240.

[9] Wan M, Yin W, Zhang WH. Study on the correction of cutting force measurement with table dynamometer. Procedia CIRP 2016; 56: 119–123.

[10] Wan M, Yin W, Zhang WH, Liu H. Improved inverse filter for the correction of distorted measured cutting forces. International Journal of Mechanical Sciences 2017; 120: 276–285.

[11] Mebrahitom A, Choon W, Azhari A. Side milling machining simulation using finite element analysis: Prediction of cutting forces. Materials Today: Proceedings 2017; 4(4): 5215–5221.

[12] Masmiati N, Sarhan AAD, Hassan MAN, Hamdi M. Optimization of cutting conditions for minimum residual stress, cutting force and surface roughness in end milling of S50C medium carbon steel. Journal of the International Measurement Confederation 2016; 86: 253–265.

[13] Mohd Khalil AN, Azmi AI, Murad MN, Mahboob Ali MA. The effect of cutting parameters on cutting force and tool wear in machining Nickel Titanium Shape Memory Alloy ASTM F2063 under Minimum Quantity Nanolubricant. Procedia CIRP. 2018; 77(Hpc): 227–230.

[14] Gaikhe V, Sahu J, Pawade R. Optimization of cutting parameters for cutting force minimisation in helical ball end milling of inconel 718 by using genetic algorithm. Procedia CIRP. 2018; 77(Hpc): 477–480.

[15] Caudill J, Schoop J, Jawahir IS. Numerical modeling of cutting forces and temperature distribution in high speed cryogenic and flood-cooled milling of Ti-6Al-4V. Procedia CIRP. 2019; 82: 83–88.

[16] Tsai MY, Chang SY, Hung JP, Wang CC. Investigation of milling cutting forces and cutting coefficient for aluminum 6060-T6. Computers & Electrical Engineering 2016; 51: 320–330.

[17] Liu H, Zhang J, Jiang Y, He Y, Xu X, Zhao W. Investigation on morphological evolution of chips for Ti6Al4V alloys with the increasing milling speed. Procedia CIRP 2016; 46: 408–411.

[18] Karpuschewski B, Kundrák J, Varga G, et al. Determination of specific cutting force components and exponents when applying high feed rates. Procedia CIRP. 2018; 77(Hpc): 30–33.

[19] Mohd Nor NA, Baharudin BTHT, A Ghani J, et al. Effect of chip load and spindle speed on cutting force of Hastelloy X. Journal of Mechanical Engineering and Sciences 2020; 14(1): 6497–6503.

[20] Antwi EK, Liu K, Wang H. A review on ductile mode cutting of brittle materials. Frontiers in Mechanical Engineering 2018; 13(2): 251–263.

[21] Philipp M, Yuta M, Yasuhiro K, Sangkee M. Anisotropic brittle-ductile transition of monocrystalline sapphire during orthogonal cutting and nanoindentation experiments. Nami Jishu yu Jingmi Gongcheng/Nanotechnology and Precision Engineering 2018; 1(3): 157–171.

[22] Daramola OO, Tlhabadira I, Olajide JL, et al. Process design for optimal minimisation of resultant cutting force during the machining of Ti-6Al-4V: Response surface method and desirability function analysis. Procedia CIRP. 2019; 84: 854–860.

[23] Wang B, Liu Z. Investigations on deformation and fracture behavior of workpiece material during high speed machining of 7050-T7451 aluminum alloy. CIRP Journal of Manufacturing Science and Technology 2016; 14: 43–54.

[24] Ajeet Vasant J, Gopi G, John Rozario Jegaraj J, et al. Finite element simulation and experimental validation of laser assisted machining of Inconel 718. Materials Today: Proceedings 2018; 5(Part 2): 13637–13649.

[25] Zhang Q, Zhang S, Li J. Three dimensional finite element simulation of cutting forces and cutting temperature in hard milling of AISI H13 Steel. Procedia Manufacturing 2017; 10: 37–47.